

A POSTERIORI ERROR ANALYSIS OF A CELL-CENTERED FINITE VOLUME METHOD FOR SEMILINEAR ELLIPTIC PROBLEMS

DON ESTEP ^{*}, MICHAEL PERNICE [†], DU PHAM [‡], SIMON TAVENER [§], AND
HAIYING WANG [¶]

Abstract. In this paper, we conduct a goal-oriented *a posteriori* analysis for the error in a quantity of interest computed from a cell-centered finite volume scheme for a semilinear elliptic problem. The *a posteriori* error analysis is based on variational analysis, residual errors and the adjoint problem. To carry out the analysis, we use an equivalence between the cell-centered finite volume scheme and a mixed finite element method with special choice of quadrature.

Key words. *a posteriori* error analysis, adjoint problem, cell-centered finite volume method, convection-diffusion-reaction problem, mixed finite element method, quadrature error, residual error

AMS subject classifications. 65N06 65N15

1. Introduction. Evaluating the predictive capability of numerical simulation of a complex physical model requires quantification and control of numerical and modeling errors. Over the last two decades, there has been substantial development of goal-oriented *a posteriori* error estimation based on duality and adjoint operators for finite element methods, see [14, 12, 13, 16, 5, 18, 8] and the references therein. However, the application of this approach to popular finite difference and finite volume methods has lagged behind. Part of the problem is that these approaches do not fit into a variational framework as naturally as finite element methods.

Our particular interest is in finite volume schemes, which are especially useful for solving partial differential equations that represent conservation laws. Many examples can be identified in fields such as computational fluid dynamics, magnetohydrodynamics, heat transfer, and flow in porous media since their derivation, which is based on the integral formulation of conservation laws, yields a discretization that locally preserves conservation at the discrete level. The similarity of this approach to the weak formulation led to early observation of the ability of finite volume methods to faithfully reproduce weak solutions that are only piecewise smooth, such as shocks [23, 24]. Moreover, finite volume discretizations are relatively simple to implement.

There has been considerable work on convergence analysis of finite volume methods (see [17] for an extensive review). Classical analysis of discretization methods for partial differential equations tends to focus on estimating the error in global norms, such as the L^2 and energy norms. In practice, however, this may not be meaningful.

^{*}Department of Mathematics, Department of Statistics, Colorado State University, Fort Collins, CO 80524, USA, email: estep@math.colostate.edu. Research is supported in part by the Department of Energy (DE-FG02-04ER25620, DE-FG02-05ER25699, DE-FC02-07ER54909), the National Aeronautics and Space Administration (NNG04GH63G), the National Science Foundation (DMS-0107832, DMS-0715135, DGE-0221595003, MSPA-CSE-0434354, ECCS-0700559), Idaho National Laboratory (00069249), and the Sandia Corporation (PO299784).

[†]Idaho National Laboratory, Idaho Falls, ID 83415, USA, email: Michael.Pernice@inl.gov.

[‡]Department of Mathematics, Colorado State University, Fort Collins, CO 80524, USA, email: pham@math.colostate.edu. Research is supported in part by the Department of Energy DE-FC02-07ER54909.

[§]Department of Mathematics, Colorado State University, Fort Collins, CO 80524, USA, email: tavener@math.colostate.edu.

[¶]Department of Mathematics, Colorado State University, Fort Collins, CO 80524, USA, email: wangh@math.colostate.edu. Research is supported in part by the Idaho National Laboratory (00069249).

Often, the practical goal for solving a differential equation is to compute specific information from the solution. In that situation, the concern is the error in the desired information, which may not have much to do with the error in some global norm. In contrast, the goal of the *a posteriori* error analysis conducted below is to estimate the error in a quantity of interest that can be represented as a linear functional, e.g. the average error over some subdomain or the error at a point or along a line segment.

We note that there are other kinds of *a posteriori* error analysis. In particular, there is an extensive literature on the derivation of *a posteriori* error bounds, usually targeted for the energy norm. The error in the energy norm may or may not have much to do with the error in particular quantity of interest, and generically error bounds are much larger than error estimates that allow for the effects of cancellation of error. On the other hand, *a posteriori* error bounds have the benefits of yielding provable upper bounds and optimal order dependence on discretization parameters.

The literature on *a posteriori* error analysis for finite volume methods is relatively slim compared to that for finite element methods. In terms of goal-oriented estimates, T. Barth [7] derives *a posteriori* error estimates for hyperbolic conservation laws with specialized variants given for the Godunov finite volume and discontinuous Galerkin finite element methods. A *a posteriori* error estimation for Godunov finite volume methods and discontinuous Galerkin methods is given in [22] and [21] by Larson and Barth. In terms of *a posteriori* error bounds for finite volume schemes, see for example [11, 3, 19, 29, 30, 26, 25, 10, 1, 2].

In this paper, we analyze the cell-centered finite volume scheme applied to a convection-diffusion-reaction problem. The *a posteriori* estimate derived in this paper involves variational analysis, computable residuals to measure local introduction of error, and the generalized Green's function solving the adjoint problem to quantify the global effects of accumulation and propagation of error in the quantity of interest. The resulting estimate is very accurate, even on coarse meshes. In order to use variational analysis and the adjoint operator, we employ an equivalence between the finite volume method and the lowest order Raviart-Thomas mixed finite method with special quadrature derived in [28] for elliptic problems with homogeneous Dirichlet boundary conditions. This equivalence is well-known in the finite element community, but is apparently less well-known in the wider engineering and science communities that employ finite volume methods. We expand the known equivalence between the two methods to include convection-diffusion-reaction problems with nonhomogeneous Dirichlet and Neumann boundary conditions. We then carry out the *a posteriori* analysis on the lowest order Raviart-Thomas mixed method and hence derive an error representation for the equivalent finite volume scheme.

The paper is organized as follows. In §2, we review the Raviart-Thomas mixed finite element method for convection-diffusion problems with nonhomogeneous boundary conditions. In §3, a cell-centered finite volume scheme is constructed. In §4, the finite volume scheme is reformulated as a mixed method and the analogy between the finite element and finite volume methods is then made. The *a posteriori* analysis is performed in §5 and the accuracy of the estimates produced is demonstrated by the numerical experiments reported in §6. We present our conclusions in §7. Some derivations and proofs are given in §8.

2. The mixed finite element method. In the general case, we consider the convection-diffusion-reaction problem with mixed Dirichlet-Neumann boundary con-

ditions,

$$\begin{cases} -\nabla \cdot (a\nabla p + \boldsymbol{\beta} p) = f, & \text{in } \Omega, \\ p = \mathbf{g}_D, & \text{on } \Gamma_D, \\ -a\nabla p \cdot \mathbf{n} = \mathbf{g}_N, & \text{on } \Gamma_N, \end{cases} \quad (2.1)$$

where $\Omega \in \mathbb{R}^N$ is a convex polyhedral domain ($N \geq 2$) with boundary $\partial\Omega$. In this paper, for simplicity, we take Ω to be a unit square in \mathbb{R}^2 , with $\Gamma_D = \{(0, y), (x, 0), x, y \in [0, 1]\}$ and $\Gamma_N = \partial\Omega \setminus \Gamma_D = \{(1, y), (x, 1), x, y \in [0, 1]\}$. We can treat other combinations of boundary conditions in an obvious way. We assume that $\boldsymbol{\beta} = (\boldsymbol{\beta}^x, \boldsymbol{\beta}^y)^\top$ is smooth, $a(\mathbf{x})$ is bounded below by a positive number, $f = f(p) \in L^2(\Omega)$ is Lipschitz continuous with respect to p , $\mathbf{g}_D \in H^{1/2}(\Gamma_D)$, $\mathbf{g}_N \in H^{-1/2}(\Gamma_N)$. Moreover, we assume that convection coefficient $\boldsymbol{\beta}$ satisfies that $|\boldsymbol{\beta}|$ is sufficiently small with respect to a . Otherwise, some form of stabilization might be required.

To formulate the mixed finite element (MFE) scheme, we follow [20] and rewrite (2.1) as a first order system by setting $\mathbf{u} = -(a\nabla p + \boldsymbol{\beta} p)$ in (2.1) to obtain

$$\begin{cases} a^{-1}\mathbf{u} + \nabla p + \mathbf{b}p = \mathbf{0}, & \text{in } \Omega, \\ \nabla \cdot \mathbf{u} = f, & \text{in } \Omega, \\ p = \mathbf{g}_D, & \text{on } \Gamma_D, \\ \mathbf{u} \cdot \mathbf{n} + \boldsymbol{\beta} \cdot \mathbf{n} p = \mathbf{g}_N, & \text{on } \Gamma_N, \end{cases} \quad (2.2)$$

where $\mathbf{b} = a^{-1}\boldsymbol{\beta}$. We assume that $p \in W = L^2(\Omega)$, $\mathbf{u} \in \mathbf{V} = \mathbf{H}(\text{div}; \Omega) = \{\mathbf{v} \in (L^2(\Omega))^2 : \text{div } \mathbf{v} \in L^2(\Omega)\}$. Note that the Neumann boundary condition in the original problem becomes a Robin condition in the new system. In the case of a nonempty Neumann boundary, we introduce an auxiliary variable, the so-called Lagrange multiplier $\lambda \in M = H^{1/2}(\Gamma_N)$, see [4], to represent the pressure on Neumann boundary edges. The variational form for the true solution is

$$(a^{-1}\mathbf{u}, \mathbf{v})_\Omega - (p, \nabla \cdot \mathbf{v})_\Omega + (\mathbf{b}p, \mathbf{v})_\Omega + \langle \lambda, \mathbf{v} \cdot \mathbf{n} \rangle_{\Gamma_N} = -\langle \mathbf{g}_D, \mathbf{v} \cdot \mathbf{n} \rangle_{\Gamma_D}, \quad (2.3a)$$

$$(\nabla \cdot \mathbf{u}, w)_\Omega = (f, w)_\Omega, \quad (2.3b)$$

$$\langle \mathbf{u} \cdot \mathbf{n} + \boldsymbol{\beta} \cdot \mathbf{n} \lambda, \mu \rangle_{\Gamma_N} = \langle \mathbf{g}_N, \mu \rangle_{\Gamma_N}, \quad (2.3c)$$

for all $(\mathbf{v}, w, \mu) \in (\mathbf{V}, W, M)$. Here, $(\cdot, \cdot)_D$ and $\langle \cdot, \cdot \rangle_\gamma$ denote inner products on $D \subset \mathbb{R}^2$ and lower order domain $\gamma \subset \mathbb{R}$. Notice that if $p \in H^1(\Omega)$, $\lambda \in H^{1/2}(\Omega)$ is simply the trace of p on Neumann boundary. We let Ω_h denote a quadrilateralization of Ω . We construct specially designed finite-dimensional subspaces on Ω_h ,

$$\mathbf{V}_h \subset \mathbf{V}, \quad W_h \subset W, \quad M_h \subset M.$$

The finite element method is then: Compute $(\mathbf{u}_h, p_h, \lambda_h) \in (\mathbf{V}_h, W_h, M_h)$ satisfying

$$\begin{aligned} (a^{-1}\mathbf{u}_h, \mathbf{v})_{\Omega_h} - (p_h, \nabla \cdot \mathbf{v})_{\Omega_h} + (\mathbf{b}p_h, \mathbf{v})_{\Omega_h} + \langle \lambda_h, \mathbf{v} \cdot \mathbf{n} \rangle_{\Gamma_N} \\ = -\langle \mathbf{g}_D, \mathbf{v} \cdot \mathbf{n} \rangle_{\Gamma_D}, \end{aligned} \quad (2.4a)$$

$$(\nabla \cdot \mathbf{u}_h, w)_{\Omega_h} = (f, w)_{\Omega_h}, \quad (2.4b)$$

$$\langle \mathbf{u}_h \cdot \mathbf{n} + \boldsymbol{\beta} \cdot \mathbf{n} \lambda_h, \mu \rangle_{\Gamma_N} = \langle \mathbf{g}_N, \mu \rangle_{\Gamma_N}, \quad (2.4c)$$

for all $(\mathbf{v}, w, \mu) \in (\mathbf{V}_h, W_h, M_h)$. Here $(\sigma, \tau)_{\Omega_h} = \sum_{K \in \Omega_h} (\sigma, \tau)_K$. The subscripts of integrals over Ω_h are omitted unless there is ambiguity.

It is known that \mathbf{V}_h and W_h need to satisfy certain properties to guarantee convergence. One condition is $\operatorname{div} \mathbf{V}_h \subset W_h$. The following space by Raviart and Thomas is devised to meet that purpose. Before proceeding, we introduce some notation. For a partition Δ of $[0, 1]$, and for $r = 0, 1, 2, \dots, q = -1, 0, 1, \dots$, we define the piecewise-polynomial space $\mathfrak{M}_q^r(\Delta) = \{v \in C^q([0, 1]): v \text{ is a polynomial of degree } \leq r \text{ on each subinterval of } \Delta\}$. When $q = -1$, the functions are discontinuous. Thus, the space of continuous piecewise bi-linear functions on the unit square is the tensor-product space $\mathfrak{M}_0^1(\Delta_x) \otimes \mathfrak{M}_0^1(\Delta_y)$. Let

$$\begin{aligned} W_h^r &= \mathfrak{M}_{-1}^r(\Delta_x) \otimes \mathfrak{M}_{-1}^r(\Delta_y); \\ \mathbf{V}_h^r &= [\mathfrak{M}_0^{r+1}(\Delta_x) \otimes \mathfrak{M}_{-1}^r(\Delta_y)] \times [\mathfrak{M}_{-1}^r(\Delta_x) \otimes \mathfrak{M}_0^{r+1}(\Delta_y)]. \end{aligned}$$

When $r = 0$, we obtain the following two spaces for the lowest order Raviart-Thomas MFE scheme. Let $W_h = W_h^0$ which is a space of piecewise constant functions and $\mathbf{V}_h = \mathbf{V}_h^0$ which is a space of vector-valued functions whose x -components are continuous linear in x and discontinuous constant in y and whose y -components are discontinuous constant in x and continuous linear in y . In the lowest order case, the space M_h for the Lagrange multipliers consists of piecewise constant functions on Neumann boundary edges.

To express Galerkin orthogonality, we use the Raviart-Thomas projection on quadrilateral elements. Denote

$$P_{k1,k2}(K) = \left\{ p(x, y) = \sum_{i \leq k1; j \leq k2} c_{ij} x^i y^j, \quad (x, y) \in K, \quad c_{ij} \in \mathbb{R} \right\}$$

for $K \in \Omega_h$. The k -th order Raviart-Thomas space is

$$\mathbf{V}_{\text{RT}}^k(K) = P_{k+1,k}(K) \times P_{k,k+1}(K).$$

The k -th order Raviart-Thomas projection $\Pi_h : \mathbf{V}|_K \mapsto \mathbf{V}_{\text{RT}}^k(K)$ is, for $\mathbf{v} \in \mathbf{V}|_K$,

$$\langle (\Pi_h \mathbf{v} - \mathbf{v}) \cdot \mathbf{n}, z \rangle_e = 0, \quad \forall z \in \mathcal{P}^k(e), \quad \forall e \in \partial K, \quad (2.5a)$$

$$(\Pi_h \mathbf{v} - \mathbf{v}, \boldsymbol{\eta})_K = 0, \quad \forall \boldsymbol{\eta} \in \mathbf{V}_{\text{RT}}^{k-1}(K). \quad (2.5b)$$

From the definition of Π_h , we have that, [9], for $\mathbf{v} \in \mathbf{V}|_K$,

$$(\nabla \cdot (\Pi_h \mathbf{v} - \mathbf{v}), w)_K = 0, \quad \forall w \in W_h|_K; \quad (2.6)$$

$$\|\Pi_h \mathbf{v} - \mathbf{v}\|_{0,K} \leq C \|\mathbf{v}\|_{k+1,K} h^{k+1}; \quad (2.7)$$

$$\|\nabla \cdot (\Pi_h \mathbf{v} - \mathbf{v})\|_{0,K} \leq C \|\nabla \cdot \mathbf{v}\|_{k+1,K} h^{k+1}, \quad (2.8)$$

if \mathbf{v} has the required smoothness. Here, the usual norm notation $\|\cdot\|_{m,D}$ for space $H^m(D)$ is adopted, m is an integer and $D \subset \mathbb{R}^2$. We also need the $L^2(\Omega)$ -projection, \mathbb{P}_h , from W to W_h with

$$\|\mathbb{P}_h w - w\|_{0,K} \leq C \|w\|_{k+1,K} h^{k+1}, \quad \forall K \in \Omega_h. \quad (2.9)$$

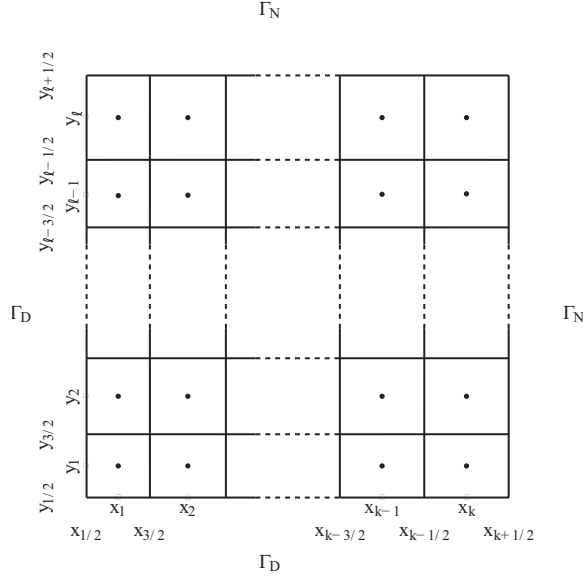


FIG. 3.1. The cell centered grid of Ω .

3. A cell-centered finite volume scheme. We now introduce the grid for the cell-centered finite volume scheme for which we partition Ω in the x - and y - directions as

$$0 = x_{1/2} < x_1 < x_{3/2} < x_2 < \dots < x_{k-1/2} < x_k < x_{k+1/2} = 1;$$

$$0 = y_{1/2} < y_1 < y_{3/2} < y_2 < \dots < y_{\ell-1/2} < y_\ell < y_{\ell+1/2} = 1.$$

We then define the cells (finite volumes) to be the rectangles $K_{ij} = (x_{i-1/2}, x_{i+1/2}) \times (y_{j-1/2}, y_{j+1/2})$, $i = 1, \dots, k$, $j = 1, \dots, \ell$ with the centers (x_i, y_j) and nodes of half indices. Denote

$$\Delta x_{i+1/2} = x_{i+1} - x_i, \quad i = 1, \dots, k-1; \quad \Delta x_i = x_{i+1/2} - x_{i-1/2}, \quad i = 1, \dots, k;$$

$$\Delta y_{j+1/2} = y_{j+1} - y_j, \quad j = 1, \dots, \ell-1; \quad \Delta y_j = y_{j+1/2} - y_{j-1/2}, \quad j = 1, \dots, \ell.$$

The discrete cell-centered finite volume mesh Ω_h is then defined as follows (see Fig. 3.1),

$$\Omega_h = \{K_{ij}, \quad i = 1, \dots, k; \quad j = 1, \dots, \ell\}.$$

In this paper, we construct the scheme and derive the analysis on a rectangular mesh for simplicity. Some modifications are required to extend our analysis to non-rectangular meshes.

To enforce the boundary conditions across the outer boundaries, we define the fictitious boundary cells where the ghost values $\{p_{0,j}, p_{k+1,j}, j = 1, \dots, \ell\}$ and

$\{p_{i,0}, p_{i,\ell+1}, i = 1, \dots, k\}$ are defined. We set

$$\begin{aligned} K_{0j} &= (x_{-1/2}, x_{1/2}) \times (y_{j-1/2}, y_{j+1/2}), \\ K_{k+1j} &= (x_{k+1/2}, x_{k+3/2}) \times (y_{j-1/2}, y_{j+1/2}), \\ K_{i0} &= (x_{i-1/2}, x_{i+1/2}) \times (y_{-1/2}, y_{1/2}), \\ K_{i\ell+1} &= (x_{i-1/2}, x_{i+1/2}) \times (y_{\ell+1/2}, y_{\ell+3/2}), \end{aligned}$$

where $i = 1, \dots, k$, $j = 1, \dots, \ell$, and

$$\begin{aligned} x_{-1/2} &= -x_{3/2}, & x_{k+3/2} &= 2 - x_{k-1/2}, \\ y_{-1/2} &= -y_{3/2}, & y_{\ell+3/2} &= 2 - y_{\ell-1/2}. \end{aligned}$$

We are then able to discretize (2.1) by the following finite volume scheme

$$\begin{aligned} & -\Delta y_j (a_{i+1/2,j} \delta_x p_{i+1/2,j} - a_{i-1/2,j} \delta_x p_{i-1/2,j}) \\ & -\Delta x_i (a_{i,j+1/2} \delta_y p_{i,j+1/2} - a_{i,j-1/2} \delta_y p_{i,j-1/2}) \\ & -\Delta y_j \left(\beta_{i+1/2,j}^x \hat{p}_{i+1/2,j} - \beta_{i-1/2,j}^x \hat{p}_{i-1/2,j} \right) \\ & -\Delta x_i \left(\beta_{i,j+1/2}^y \hat{p}_{i,j+1/2} - \beta_{i,j-1/2}^y \hat{p}_{i,j-1/2} \right) = f_{ij} \Delta x_i \Delta y_j, \end{aligned} \quad (3.1)$$

for $1 \leq i \leq k$, $1 \leq j \leq \ell$. Here, we use $\delta_x p$ ($\delta_y p$) to denote an approximation to $\partial p / \partial x$ ($\partial p / \partial y$) and \hat{p} represents an approximation to the pressure in convection term. The definitions and the derivation for this specific scheme are given in §8.1.

The scheme (3.1) agrees with the discretization of FV schemes in [6] which differs from the classical schemes, see e.g. [17], in the way we compute the coefficients a . Here, a takes the value at the corresponding cell boundary while in the classical scheme it takes the harmonic average values of the adjacent cells. The *a posteriori* analysis can be extended to cover the traditional scheme.

We now rewrite (3.1) in a form that can be related to the MFE scheme described in the next section. To this end, we define

$$\begin{aligned} \mathbf{u}_{i+1/2,j}^x &= -a_{i+1/2,j} \delta_x p_{i+1/2,j} - \beta_{i+1/2,j}^x \hat{p}_{i+1/2,j}, & 0 \leq i \leq k, & 1 \leq j \leq \ell, \\ \mathbf{u}_{i,j+1/2}^y &= -a_{i,j+1/2} \delta_y p_{i,j+1/2} - \beta_{i,j+1/2}^y \hat{p}_{i,j+1/2}, & 1 \leq i \leq k, & 0 \leq j \leq \ell, \end{aligned}$$

where $\delta_x p$, $\delta_y p$ and \hat{p} are defined in (8.2), (8.3) and (8.6), respectively. Using this notation, the ‘‘mixed’’ form of (3.1) becomes

$$\mathbf{u}_{i+1/2,j}^x + a_{i+1/2,j} \delta_x p_{i+1/2,j} + \beta_{i+1/2,j}^x \hat{p}_{i+1/2,j} = 0, \quad 0 \leq i \leq k, 1 \leq j \leq \ell, \quad (3.2a)$$

$$\mathbf{u}_{i,j+1/2}^y + a_{i,j+1/2} \delta_y p_{i,j+1/2} + \beta_{i,j+1/2}^y \hat{p}_{i,j+1/2} = 0, \quad 1 \leq i \leq k, 0 \leq j \leq \ell, \quad (3.2b)$$

$$\begin{aligned} \Delta y_j \left(\mathbf{u}_{i+1/2,j}^x - \mathbf{u}_{i-1/2,j}^x \right) + \Delta x_i \left(\mathbf{u}_{i,j+1/2}^y - \mathbf{u}_{i,j-1/2}^y \right) &= f_{ij} \Delta x_i \Delta y_j, \\ & 1 \leq i \leq k, 1 \leq j \leq \ell, \end{aligned} \quad (3.2c)$$

with the Neumann boundary condition of (8.5) becoming

$$\mathbf{u}_{k+1/2,j}^x + \beta_{k+1/2,j}^x \lambda_{k+1/2,j}^{\text{FV}} = (\mathbf{g}_N)_{k+1/2,j}, \quad (3.3a)$$

$$\mathbf{u}_{i,\ell+1/2}^y + \beta_{i,\ell+1/2}^y \lambda_{i,\ell+1/2}^{\text{FV}} = (\mathbf{g}_N)_{i,\ell+1/2}, \quad (3.3b)$$

for $1 \leq i \leq k$, $1 \leq j \leq \ell$, where λ^{FV} denotes edge pressure approximation on Γ_{N} .

Even though we have obtained a formulation in terms of both p_h and \mathbf{u}_h , we do not have an approximation to velocity \mathbf{u} everywhere in the interior of each cell. Instead, substituting the piecewise constant pressure approximation into (3.2a) and (3.2b) provides a flux approximation, \mathbf{u}_h^x and \mathbf{u}_h^y , across the interfaces. Recall that the lowest order Raviart-Thomas velocity is of the form $P_{1,0} \times P_{0,1}$, that is, x -component being linear in x and constant in y and y -component linear in y and constant in x . So a linear combination of fluxes \mathbf{u}_h^x and \mathbf{u}_h^y along x - or y - direction makes a reasonable approximation to \mathbf{u} . This is equivalent to recovering \mathbf{u}_h from \mathbf{u}_h^x and \mathbf{u}_h^y using the lowest order Raviart-Thomas projection (2.5). Obviously, the property of conservation is preserved during the process.

4. Analogy between MFE and FV. We next state the analogy between the mixed method of lowest order and cell-centered finite differences to illuminate the connection between the FV and MFE schemes (see [28]):

LEMMA 4.1. *If $(\mathbf{u}_h, p_h, \lambda_h) \in \mathbf{V}_h \times W_h \times M_h$ satisfies (3.2) and (3.3), then it also satisfies (2.4) in the following way*

$$\begin{aligned} & (a^{-1}\mathbf{u}_h^x, \mathbf{v}^x)_{T_x M_y} + (a^{-1}\mathbf{u}_h^y, \mathbf{v}^y)_{M_x T_y} - (p_h, \nabla \cdot \mathbf{v}) \\ & + (\mathbf{b}^x p_h, \mathbf{v}^x)_{T_x M_y} + (\mathbf{b}^y p_h, \mathbf{v}^y)_{M_x T_y} + \langle \lambda_h, \mathbf{v} \cdot \mathbf{n} \rangle_{\Gamma_{\text{N}}} = - \langle \mathbf{g}_{\text{D}}, \mathbf{v} \cdot \mathbf{n} \rangle_{\Gamma_{\text{D}, M}}, \end{aligned} \quad (4.1a)$$

$$(\nabla \cdot \mathbf{u}_h, w) = (f, w)_{M_x M_y}, \quad (4.1b)$$

$$\langle \mathbf{u}_h \cdot \mathbf{n} + \boldsymbol{\beta} \cdot \mathbf{n} \lambda_h, \mu \rangle_{e, M} = \langle \mathbf{g}_{\text{N}}, \mu \rangle_{e, M}, \quad (4.1c)$$

for any $\mathbf{v} \in \mathbf{V}_h$, $w \in W_h$ and $\mu \in M_h$. Here, $T_x(T_y)$ and $M_x(M_y)$ represent trapezoidal and midpoint quadrature rules in $x(y)$ - direction. With no subscript, M indicates midpoint approximation on cell edges.

A detailed proof is given in §8.2. This shows that the cell-centered FV scheme and the lowest order Raviart-Thomas MFE scheme with the use of specific quadrature rules are equivalent in the sense of producing the same discrete values at the centers of the cells. The Raviart-Thomas MFE method, with a proper choice of basis functions for \mathbf{u}_h , p_h and λ_h , yields a linear system of the form

$$\begin{pmatrix} A & B & C \\ E & 0 & 0 \\ T & 0 & S \end{pmatrix} \begin{pmatrix} U \\ P \\ \Lambda \end{pmatrix} = \begin{pmatrix} F \\ G \\ L \end{pmatrix}, \quad (4.2)$$

where U , P , Λ are the vectors of degrees of freedom associated with \mathbf{u}_h , p_h and λ_h , respectively. The quadrature rules have a strong impact on the linear system corresponding to the mixed FV scheme. Since the special quadratures allow \mathbf{u}_h and p_h variables to be decoupled, an equivalent block form of the cell-centered FV scheme is

$$\begin{pmatrix} \mathbb{A} & \mathbb{B} & \mathbb{C} \\ 0 & \mathbb{D} & 0 \\ \mathbb{T} & 0 & \mathbb{S} \end{pmatrix} \begin{pmatrix} \mathbb{U} \\ \mathbb{P} \\ \bar{\Lambda} \end{pmatrix} = \begin{pmatrix} \mathbb{F} \\ \mathbb{G} \\ \mathbb{L} \end{pmatrix}, \quad (4.3)$$

where only the sub-system $\mathbb{D}\mathbb{P} = \mathbb{G}$ is actually solved in practice. It is interesting to compare these two systems. For an elliptic problem with no convection and diffusion coefficient $a \equiv 1$, we compute the condition numbers of the matrix of (4.2) and the sub-matrix \mathbb{D} of (4.3), listed in Table 4.1. The first column, grid level, indicates

TABLE 4.1
Condition numbers and their increasing rates of FV and MFE schemes for different mesh levels

grid level	FV		MFE	
	cond	rate	cond	rate
1	1.00	–	13.00	–
2	2.00	1.00	28.00	1.11
3	9.00	2.17	68.62	1.29
4	37.26	2.05	165.16	1.27
5	150.26	2.01	378.54	1.20
6	603.05	2.00	883.05	1.22

the mesh size $h = 1/2^n$, $n = 1, \dots, 6$. As expected, the FV scheme has a smaller condition number than that of the MFE scheme at the same mesh level. But the difference in the condition numbers lessens as mesh is refined.

5. An *a posteriori* error analysis. We now conduct an *a posteriori* error analysis for the cell-centered finite volume method in (4.1), by exploiting its equivalent representation as a mixed finite element scheme with particular quadrature rules. First, we define the errors $\mathbf{e}_\mathbf{u} = \mathbf{u} - \mathbf{u}_h$ of \mathbf{u} , $e_p = p - p_h$ of p and $e_\lambda = \lambda - \lambda_h$ of λ , where \mathbf{u} , p and λ are not known in general. We next derive the equations for these errors by subtracting (4.1a), (4.1b) and (4.1c) from the first, second and third equation of (2.3) respectively, yielding

$$(a^{-1}e_\mathbf{u}, \mathbf{v}) - (e_p, \nabla \cdot \mathbf{v}) + (\mathbf{b}e_p, \mathbf{v}) + \langle e_\lambda, \mathbf{v} \cdot \mathbf{n} \rangle_{\Gamma_N} = \text{QE1}(\mathbf{v}), \quad \forall \mathbf{v} \in V_h, \quad (5.1a)$$

$$(\nabla \cdot e_\mathbf{u}, w) - \left(\overline{f'(p, p_h)} e_p, w \right) = \text{QE2}(w), \quad \forall w \in W_h, \quad (5.1b)$$

$$\langle e_\mathbf{u} \cdot \mathbf{n} + \boldsymbol{\beta} \cdot \mathbf{n} e_\lambda, \mu \rangle_{\Gamma_N} = \text{QE3}(\mu), \quad \forall \mu \in M_h, \quad (5.1c)$$

where $\overline{f'(p, p_h)} = \int_0^1 f'(sp + (1-s)p_h) ds$ and $\overline{f'(p, p_h)} e_p = f(p) - f(p_h)$, and QE1, QE2 and QE3 are the quadrature errors defined as

$$\begin{aligned} \text{QE1}(\mathbf{v}) = & - (a^{-1}\mathbf{u}_h, \mathbf{v}) + \left((a^{-1}\mathbf{u}_h^x, \mathbf{v}^x)_{T_x M_y} + (a^{-1}\mathbf{u}_h^y, \mathbf{v}^y)_{M_x T_y} \right) \\ & - (\mathbf{b}p_h, \mathbf{v}) + \left((\mathbf{b}^x p_h, \mathbf{v}^x)_{T_x M_y} + (\mathbf{b}^y p_h, \mathbf{v}^y)_{M_x T_y} \right) \\ & - \langle \mathbf{g}_D, \mathbf{v} \cdot \mathbf{n} \rangle_{\Gamma_D} + \langle \mathbf{g}_D, \mathbf{v} \cdot \mathbf{n} \rangle_{\Gamma_D, M}; \end{aligned} \quad (5.2)$$

$$\text{QE2}(w) = (f(p_h), w) - (f(p_h), w)_{M_x M_y}; \quad (5.3)$$

$$\text{QE3}(\mu) = \left(\langle \mathbf{g}_N, \mu \rangle_{\Gamma_N} - \langle \mathbf{g}_N, \mu \rangle_{\Gamma_N, M} \right) + \left(\langle \boldsymbol{\beta} \cdot \mathbf{n} \lambda_h, \mu \rangle_{\Gamma_N, M} - \langle \boldsymbol{\beta} \cdot \mathbf{n} \lambda_h, \mu \rangle_{\Gamma_N} \right). \quad (5.4)$$

We now state the main result as follows:

THEOREM 5.1. *Suppose e_p , $\mathbf{e}_\mathbf{u}$ and e_λ satisfy the error equations (5.1) for problem (2.1) and its finite volume scheme (3.1). For any $\psi_1 \in (L^2(\Omega))^2$ and $\psi_2 \in L^2(\Omega)$, the quantity of interests expressed as linear functionals i.e., $(e_p, \psi_2) + (\mathbf{e}_\mathbf{u}, \psi_1)$ can*

be computed as follows

$$\begin{aligned}
& (e_p, \psi_2) + (\mathbf{e}_u, \psi_1) \\
&= \left\{ - (a^{-1} \mathbf{u}_h, \phi_2 - \Pi_h \phi_2) - (\mathbf{b} p_h, \phi_2 - \Pi_h \phi_2) + (f(p_h), \phi_1 - \mathbb{P}_h \phi_1) \right\} \\
&\quad \left\{ - \langle \lambda_h, (\phi_2 - \Pi_h \phi_2) \cdot \mathbf{n} - \boldsymbol{\beta} \cdot \mathbf{n} (\phi_1 - \mathbb{P}_h \phi_1) \rangle_{\Gamma_N} - \langle \mathbf{g}_N - \mathbf{u}_h \cdot \mathbf{n}, \phi_1 - \mathbb{P}_h \phi_1 \rangle_{\Gamma_N} \right. \\
&\quad \left. - \langle \mathbf{g}_D, (\phi_2 - \Pi_h \phi_2) \cdot \mathbf{n} \rangle_{\Gamma_D} \right\} + \text{QE1}(\Pi_h \phi_2) + \text{QE2}(\mathbb{P}_h \phi_1) - \text{QE3}(\mathbb{P}_h \phi_1),
\end{aligned} \tag{5.5}$$

where ψ_1 and ψ_2 are solutions to the adjoint (see [15]) of (2.2) and satisfy

$$\begin{cases} a^{-1} \phi_2 - \nabla \phi_1 = \psi_1, & \text{in } \Omega, \\ -\nabla \cdot \phi_2 + \mathbf{b} \cdot \phi_2 - \overline{f'(p, p_h)}^\top \phi_1 = \psi_2, & \text{in } \Omega, \\ \langle \phi_1, \mathbf{v} \cdot \mathbf{n} \rangle_{\Gamma_D} = 0, & \text{on } \Gamma_D, \forall \mathbf{v} \in \mathbf{H}(\text{div}; \Omega), \\ \langle \boldsymbol{\beta} \cdot \mathbf{n} \phi_1 - \phi_2 \cdot \mathbf{n}, w \rangle_{\Gamma_N} = 0, & \text{on } \Gamma_N, \forall w \in H^{1/2}(\partial\Omega), \end{cases} \tag{5.6}$$

and $\phi_1 \in H^1(\Omega)$, $\phi_2 \in \mathbf{H}(\text{div}; \Omega)$.

Proof. Using (5.1a), (5.1b), (5.1c) and (5.6), and employing Galerkin orthogonality we have

$$\begin{aligned}
& (e_p, \psi_2) + (\mathbf{e}_u, \psi_1) \\
&= - (e_p, \nabla \cdot \phi_2) + (e_p, \mathbf{b} \cdot \phi_2) - \left(e_p, \overline{f'(p, p_h)}^\top \phi_1 \right) + (\mathbf{e}_u, a^{-1} \phi_2) - (\mathbf{e}_u, \nabla \phi_1) \\
&= - (e_p, \nabla \cdot (\phi_2 - \Pi_h \phi_2)) + (\mathbf{b} e_p, \phi_2 - \Pi_h \phi_2) - \left(\overline{f'(p, p_h)} e_p, \phi_1 - \mathbb{P}_h \phi_1 \right) \\
&\quad + (a^{-1} \mathbf{e}_u, \phi_2 - \Pi_h \phi_2) + (\nabla \cdot \mathbf{e}_u, \phi_1 - \mathbb{P}_h \phi_1) - \langle \mathbf{e}_u \cdot \mathbf{n}, \phi_1 \rangle_{\partial\Omega} \\
&\quad - \langle e_\lambda, \Pi_h \phi_2 \cdot \mathbf{n} \rangle_{\Gamma_N} + \text{QE1}(\Pi_h \phi_2) + \text{QE2}(\mathbb{P}_h \phi_1),
\end{aligned}$$

where Π_h and \mathbb{P}_h are defined as in (2.5) and (2.9), respectively. Hence

$$\begin{aligned}
& (e_p, \psi_2) + (\mathbf{e}_u, \psi_1) \\
&= \left\{ (a^{-1} \mathbf{u}, \phi_2 - \Pi_h \phi_2) - (p, \nabla \cdot (\phi_2 - \Pi_h \phi_2)) + (\mathbf{b} p, \phi_2 - \Pi_h \phi_2) \right\} \\
&\quad + \left\{ (\nabla \cdot \mathbf{u}, \phi_1 - \mathbb{P}_h \phi_1) - \left(\overline{f'(p, p_h)} e_p, \phi_1 - \mathbb{P}_h \phi_1 \right) \right\} \\
&\quad + \left\{ (p_h, \nabla \cdot (\phi_2 - \Pi_h \phi_2)) - (\nabla \cdot \mathbf{u}_h, \phi_1 - \mathbb{P}_h \phi_1) \right\} \\
&\quad - (a^{-1} \mathbf{u}_h, \phi_2 - \Pi_h \phi_2) - (\mathbf{b} p_h, \phi_2 - \Pi_h \phi_2) \\
&\quad - \langle \mathbf{e}_u \cdot \mathbf{n}, \phi_1 \rangle_{\partial\Omega} - \langle e_\lambda, \Pi_h \phi_2 \cdot \mathbf{n} \rangle_{\Gamma_N} \\
&\quad + \text{QE1}(\Pi_h \phi_2) + \text{QE2}(\mathbb{P}_h \phi_1).
\end{aligned}$$

By the property of Π_h , (2.6), and the definition of \mathbb{P}_h , the items in the third bracket vanish. To simplify the terms in the first two brackets, we use (2.4a) and (2.4b) and the definition of $\overline{f'(p, p_h)} e_p$, so that the error representation formula becomes

$$\begin{aligned}
& (e_p, \psi_2) + (\mathbf{e}_u, \psi_1) \\
&= \left\{ - \langle \lambda, (\phi_2 - \Pi_h \phi_2) \cdot \mathbf{n} \rangle_{\Gamma_N} - \langle \mathbf{g}_D, (\phi_2 - \Pi_h \phi_2) \cdot \mathbf{n} \rangle_{\Gamma_D} - \langle e_\lambda, \Pi_h \phi_2 \cdot \mathbf{n} \rangle_{\Gamma_N} \right. \\
&\quad \left. - \langle \mathbf{e}_u \cdot \mathbf{n}, \phi_1 \rangle_{\partial\Omega} \right\} \\
&\quad - (a^{-1} \mathbf{u}_h, \phi_2 - \Pi_h \phi_2) - (\mathbf{b} p_h, \phi_2 - \Pi_h \phi_2) + (f(p_h), \phi_1 - \mathbb{P}_h \phi_1) \\
&\quad + \text{QE1}(\Pi_h \phi_2) + \text{QE2}(\mathbb{P}_h \phi_1) \\
&=: \text{I} + \text{II} + \text{III},
\end{aligned}$$

where

$$\begin{aligned}
\text{I} &= - \langle \lambda, (\phi_2 - \Pi_h \phi_2) \cdot \mathbf{n} \rangle_{\Gamma_N} - \langle \mathbf{g}_D, (\phi_2 - \Pi_h \phi_2) \cdot \mathbf{n} \rangle_{\Gamma_D} - \langle e_\lambda, \Pi_h \phi_2 \cdot \mathbf{n} \rangle_{\Gamma_N} \\
&\quad - \langle \mathbf{e}_u \cdot \mathbf{n}, \phi_1 \rangle_{\partial\Omega} \\
\text{II} &= - (a^{-1} \mathbf{u}_h, \phi_2 - \Pi_h \phi_2) - (\mathbf{b} p_h, \phi_2 - \Pi_h \phi_2) + (f(p_h), \phi_1 - \mathbb{P}_h \phi_1) \\
\text{III} &= \text{QE1}(\Pi_h \phi_2) + \text{QE2}(\mathbb{P}_h \phi_1).
\end{aligned}$$

The terms in II represent the computable residual error of the mixed formulation approximate while III contains two quadrature errors expressions that can be approximated. The terms in I which all lie on the boundary may be analyzed further by expanding as

$$\begin{aligned}
\text{I} &= - \langle \lambda, (\phi_2 - \Pi_h \phi_2) \cdot \mathbf{n} \rangle_{\Gamma_N} - \langle e_\lambda, \Pi_h \phi_2 \cdot \mathbf{n} \rangle_{\Gamma_N} - \langle \mathbf{e}_u \cdot \mathbf{n}, \phi_1 \rangle_{\Gamma_D} \\
&\quad - \langle \mathbf{e}_u \cdot \mathbf{n}, \phi_1 \rangle_{\Gamma_N} - \langle \mathbf{g}_D, (\phi_2 - \Pi_h \phi_2) \cdot \mathbf{n} \rangle_{\Gamma_D} \\
&= - \{ \langle \lambda, \phi_2 \cdot \mathbf{n} \rangle_{\Gamma_N} + \langle \mathbf{u} \cdot \mathbf{n}, \phi_1 \rangle_{\Gamma_N} \} + \langle \lambda_h, \Pi_h \phi_2 \cdot \mathbf{n} \rangle_{\Gamma_N} + \langle \mathbf{u}_h \cdot \mathbf{n}, \phi_1 \rangle_{\Gamma_N} \\
&\quad - \langle \mathbf{g}_D, (\phi_2 - \Pi_h \phi_2) \cdot \mathbf{n} \rangle_{\Gamma_D} \\
&= - \langle \mathbf{g}_N - \mathbf{u}_h \cdot \mathbf{n}, \phi_1 \rangle_{\Gamma_N} + \langle \lambda_h, \Pi_h \phi_2 \cdot \mathbf{n} \rangle_{\Gamma_N} - \langle \mathbf{g}_D, (\phi_2 - \Pi_h \phi_2) \cdot \mathbf{n} \rangle_{\Gamma_D},
\end{aligned}$$

where we have used the adjoint boundary conditions. The third quadrature error QE3 can be extracted from the first two terms in the last equation, since

$$\begin{aligned}
&- \langle \mathbf{g}_N - \mathbf{u}_h \cdot \mathbf{n}, \phi_1 \rangle_{\Gamma_N} + \langle \lambda_h, \Pi_h \phi_2 \cdot \mathbf{n} \rangle_{\Gamma_N} \\
&= - \langle \mathbf{g}_N - \mathbf{u}_h \cdot \mathbf{n}, \phi_1 - \mathbb{P}_h \phi_1 \rangle_{\Gamma_N} - \langle \boldsymbol{\beta} \cdot \mathbf{n} \lambda_h, \mathbb{P}_h \phi_1 \rangle_{\Gamma_N} + \langle \lambda_h, \Pi_h \phi_2 \cdot \mathbf{n} \rangle_{\Gamma_N} \\
&\quad - \text{QE3}(\mathbb{P}_h \phi_1) \\
&= - \langle \mathbf{g}_N - \mathbf{u}_h \cdot \mathbf{n}, \phi_1 - \mathbb{P}_h \phi_1 \rangle_{\Gamma_N} + \langle \lambda_h, (\Pi_h \phi_2 - \phi_2) \cdot \mathbf{n} - \boldsymbol{\beta} \cdot \mathbf{n} (\mathbb{P}_h \phi_1 - \phi_1) \rangle_{\Gamma_N} \\
&\quad - \text{QE3}(\mathbb{P}_h \phi_1),
\end{aligned}$$

using (4.1c) and then applying the Neumann boundary condition of the adjoint problem. We thus obtain the error representation (5.5) with respect to the adjoint data ψ_1 and ψ_2 . \square

The following remarks highlight some of the features of this estimate:

Remark 1. The two expressions in braces in (5.5) together represent the contribution to the error arising from the finite element approximation. The last three expressions are quadrature errors, which represent the contribution to the error arising from discrete sampling of the differential operators. Due to the fact that $\Pi_h \phi_2 \cdot \mathbf{n}|_{\partial K}$ and

$\mathbb{P}_h \phi_1|_K$, $K \in \Omega_h$, are constant, the quadrature errors can be written as

$$\begin{aligned}
\text{QE1}(\Pi_h \phi_2) &= - \sum_{K \in \Omega_h} \int_K \left[a^{-1} \mathbf{u}_h^x(\Pi_h \phi_2)^x - (a^{-1} \mathbf{u}_h^x(\Pi_h \phi_2)^x)_{T_x M_y} \right] dx dy \\
&\quad - \sum_{K \in \Omega_h} \int_K \left[a^{-1} \mathbf{u}_h^y(\Pi_h \phi_2)^y - (a^{-1} \mathbf{u}_h^y(\Pi_h \phi_2)^y)_{M_x T_y} \right] dx dy \\
&\quad - \sum_{K \in \Omega_h} \int_K \left[\mathbf{b}_h^x(\Pi_h \phi_2)^x - (\mathbf{b}_h^x(\Pi_h \phi_2)^x)_{T_x M_y} \right] p_h dx dy \quad (5.7) \\
&\quad - \sum_{K \in \Omega_h} \int_K \left[\mathbf{b}_h^y(\Pi_h \phi_2)^y - (\mathbf{b}_h^y(\Pi_h \phi_2)^y)_{M_x T_y} \right] p_h dx dy \\
&\quad - \sum_{K \in \Omega_h} \int_{\partial K \cap \Gamma_D} (\mathbf{g}_D - \mathbb{I}_s \mathbf{g}_D) \Pi_h \phi_2 \cdot \mathbf{n} ds,
\end{aligned}$$

$$\text{QE2}(\mathbb{P}_h \phi_1) = \sum_{K \in \Omega_h} \int_K (f - \mathbb{I}_{xy} f) \mathbb{P}_h \phi_1 dx dy, \quad (5.8)$$

$$\text{QE3}(\mathbb{P}_h \phi_1) = \sum_{e \in \Gamma_N} \int_e (\mathbf{g}_N - \mathbb{I}_s \mathbf{g}_N) \mathbb{P}_h \phi_1 - (\boldsymbol{\beta} \cdot \mathbf{n} - \mathbb{I}_s(\boldsymbol{\beta} \cdot \mathbf{n})) \lambda_h \mathbb{P}_h \phi_1 ds. \quad (5.9)$$

where \mathbb{I}_s and \mathbb{I}_{xy} are the midpoint interpolant operators in one and two dimensions, respectively.

Remark 2. There is an essential difference between the part of the estimate that represents the effects of seeking a solution in a finite dimensional space, which can be viewed as the discretization component of the estimate, and the quadrature error terms, which represent the effect of sampling the differential operator at a finite set of points. Galerkin orthogonality holds only for the former, as evidenced by the adjoint factors consisting of the difference between the adjoint solution and its projection into the finite element spaces. It is simple to construct examples in which either component is dominant. We illustrate this in the examples of §6.

Remark 3. We now present an example to illustrate the connections between the adjoint solution and the given adjoint data. Given a forward problem with $a \equiv 1$, f linear and $\Gamma_N = \emptyset$, we choose $\psi_1 = \mathbf{0}$ and ψ_2 to be

$$\psi_2 = \begin{cases} 1, & \text{if } |x + y - 1| \leq 0.05, \\ 0, & \text{if } |x + y - 1| > 0.05. \end{cases}$$

The contours of the corresponding solutions ϕ_1 and integral curves of ϕ_2 are plotted in Fig. 5.1. In the left figure, ϕ_1 vanishes on the boundary due to the Dirichlet boundary condition specified in the forward problem. The distribution of larger values on the region around the strip $|x + y - 1| \leq 0.05$ indicates that the error in the quantity of interest is most affected by the discretization error, as reflected by the residual, and quadrature error on that region.

Remark 4. To use (5.5) to compute an estimate, we need to solve the adjoint problem numerically. Given the Galerkin orthogonality, the method used for the adjoint solution must not lie in the finite element space used for the forward problem. In fact, we essentially need to recover derivative information from the adjoint solution. In practice, we can either use a higher order method, e.g. piecewise quadratic, continuous

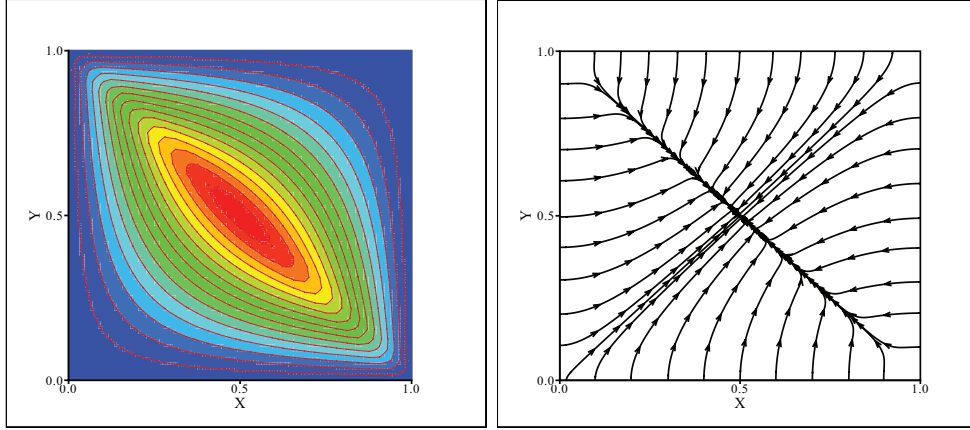


FIG. 5.1. Contour plot of ϕ_1 (left) and integral curves of ϕ_2 (right) for the adjoint problem with $a \equiv 1$, $\beta \equiv \mathbf{0}$, f being linear, $\psi_1 = \mathbf{0}$ and $\psi_2 = 1$ on the strip $|x + y - 1| \leq 0.05$ and 0 otherwise.

elements, or use the same method but computed on a finer mesh. In this paper, we solve the adjoint problem with the second order Raviart-Thomas mixed finite element method on the same mesh used for the primary computation. Specifically, the finite element spaces for the adjoint problem are taken to be

$$\mathbf{V}_{h,adj} = \{ \mathbf{v} \in \mathbf{H}(\text{div}; \Omega), \mathbf{v}|_K \in P_{2,1}(K) \times P_{1,2}(K), \forall K \in \Omega \},$$

$$W_{h,adj} = \{ w \in L^2(\Omega), w|_K \in P_1(K), \forall K \in \Omega \},$$

and

$$M_{h,adj} = \left\{ w \in H^{1/2}(\Gamma_N), \mu|_e \in P_1(e), \forall e \in \Gamma_N \right\}.$$

To enforce normal continuity of elements in $\mathbf{V}_{h,adj}$ across interior interfaces, we pick basis functions on a unit reference cell $[0, 1] \times [0, 1]$ as follows:

$$\begin{pmatrix} x-1 \\ 0 \end{pmatrix}, \begin{pmatrix} -x \\ 0 \end{pmatrix}, \begin{pmatrix} y(x-1) \\ 0 \end{pmatrix}, \begin{pmatrix} -xy \\ 0 \end{pmatrix}, \begin{pmatrix} x(x-1) \\ 0 \end{pmatrix}, \begin{pmatrix} xy(x-1) \\ 0 \end{pmatrix},$$

$$\begin{pmatrix} 0 \\ y-1 \end{pmatrix}, \begin{pmatrix} 0 \\ -y \end{pmatrix}, \begin{pmatrix} 0 \\ x(y-1) \end{pmatrix}, \begin{pmatrix} 0 \\ -xy \end{pmatrix}, \begin{pmatrix} 0 \\ y(y-1) \end{pmatrix}, \begin{pmatrix} 0 \\ xy(y-1) \end{pmatrix}.$$

The discrete weak formulations in (2.4) are then applied on $(\mathbf{V}_{h,adj}, W_{h,adj}, M_{h,adj})$ to obtain approximations to ϕ_1 and ϕ_2 . Finally, we project the approximations to the finite volume spaces by \mathbb{P}_h and Π_h to acquire approximations to $\mathbb{P}_h\phi_1$ and $\Pi_h\phi_2$.

6. Numerical tests. In this section, we demonstrate the equivalence of solutions to a cell-centered FV scheme and the MFE scheme with the special choice of quadrature and the accuracy of the *a posteriori* estimates using two examples. The quantity of interest is taken to be the average error e_p over Ω_h , which is obtained by choosing $\psi_1 = \mathbf{0}$ and $\psi_2 = 1$ in adjoint problem (5.6). Based on the discussions in Remark 4 of §5, we solve the adjoint problem on the same mesh used for the primary

TABLE 6.1
Convergence of the cell-centered FV and MFE methods.

grid level	$\ e_{p_h}^{\text{FV}}\ _\infty$		$\ e_{\mathbf{u}_h}^{\text{FV}}\ _\infty$		$\ e_{p_h}^{\text{MFE}}\ _\infty$		$\ e_{\mathbf{u}_h}^{\text{MFE}}\ _\infty$	
	error	order	error	order	error	order	error	order
1	.25e-2	–	.45e-4	–	.25e-2	–	.45e-4	–
2	.63e-3	2.00	.20e-4	1.13	.63e-3	2.00	.20e-4	1.13
3	.16e-3	2.00	.63e-5	1.71	.16e-3	2.00	.63e-5	1.71
4	.39e-4	2.00	.17e-5	1.87	.39e-4	2.00	.17e-5	1.87
5	.98e-5	2.00	.45e-6	1.94	.98e-5	2.00	.45e-6	1.94
6	.24e-5	2.00	.11e-6	1.97	.24e-5	2.00	.11e-6	1.97

TABLE 6.2
Effectivity ratio, ν , and ratio of residual errors and quadrature errors.

grid level	ν	Discrete./Quad.
1	1.0004	-.33e-3
2	1.0001	-.18e-2
3	1.0000	-.22e-2
4	1.0000	-.23e-2
5	1.0000	-.23e-2
6	1.0000	-.23e-2

computation but using the next higher order mixed finite element method so that we can evaluate the projection into the finite element space for the primary problem accurately. To evaluate the quadrature error expressions, we use a high order Gauss quadrature rule.

In the first test, $a \equiv 1$, $\beta \equiv \mathbf{0}$ and f are chosen and boundary conditions $\Gamma_D = \{0\} \times [0, 1] \cup \{1\} \times [0, 1]$, $\Gamma_N = \Omega \setminus \Gamma_D$ are imposed so that the true solution is

$$p(x, y) = \exp \left\{ -0.01 \times ((x - 0.2)^2 + (y + 0.8)^2) \right\}.$$

In Table (6.1), we list L^∞ - errors and convergence orders of two methods. The optimal order of 2 is observed. Notice also that two methods give exactly the same errors at different mesh levels. In Table (6.2), we include the effectivity ratio ν , a ratio defined as the error estimate/exact error, and a ratio of the discretization error and quadrature error components. In this example, the residual and quadrature errors both contribute to the total estimate, but the fact that the exact solution is very smooth leads to the discretization error component being much smaller than the quadrature error component.

In the second test problem, we choose $a = 2 + \sin(3\pi x) \cos(3\pi y)$, $\beta = (1.e - 4)(1, 1)^\top$, boundary conditions $\Gamma_D = \{1\} \times [0, 1] \cup [0, 1] \times \{1\}$, $\Gamma_N = \Omega \setminus \Gamma_D$, which has true solution $p(x, y) = x^5 + 4y^3$. The L^∞ - errors and convergence orders are listed in Table (6.3), and error ratios and effectivity ratio ν are listed in Table (6.4). In this example, the discretization error is the dominant error.

We note that computing *accurate* estimates depends strongly on accounting for the effects of cancellation and propagation of error throughout the domain. We illustrate in the following simple example on a unit square. The diffusion coefficient is taken to be 1 with Dirichlet boundary conditions and the true solution is

TABLE 6.3
Convergence of the cell-centered FV and MFE methods.

grid level	$\ e_{p_h}^{\text{FV}}\ _\infty$		$\ e_{\mathbf{u}_h}^{\text{FV}}\ _\infty$		$\ e_{p_h}^{\text{MFE}}\ _\infty$		$\ e_{\mathbf{u}_h}^{\text{MFE}}\ _\infty$	
	error	order	error	order	error	order	error	order
1	.24e+1	–	.35e+1	–	.24e+1	–	.35e+1	–
2	.87e+0	1.48	.95e+1	-1.43	.87e+0	1.48	.95e+1	-1.43
3	.19e+0	2.18	.23e+1	2.04	.19e+0	2.18	.23e+1	2.04
4	.53e-1	1.86	.94e+0	1.29	.53e-1	1.86	.94e+0	1.29
5	.13e-1	1.99	.33e+0	1.50	.13e-1	1.99	.33e+0	1.50
6	.33e-2	2.00	.95e-1	1.81	.33e-2	2.00	.95e-1	1.81

TABLE 6.4
Effectivity ratio, ν , and ratio of residual errors and quadrature errors.

grid level	ν	Discrete./Quad.
1	1.0722	-.17e+00
2	1.5515	-.44e+00
3	0.9355	.53e+01
4	0.9841	.71e+01
5	0.9954	.78e+01
6	0.9964	.79e+01

$p(x, y) = \sin(7\pi x) \sin(7\pi y)$. In Table. 6.5, we compare the estimate and a bound obtained by taking absolute values on each cell and then summing over the domain. As the mesh is refined and hence more cancelation occurs, the estimate is much smaller than the bound.

7. Conclusions. We have derived an *a posteriori* error estimate for a cell-centered FV scheme for convection-diffusion-reaction problems. The analysis is based on an equivalence relation between the cell-centered FV scheme and the lowest order Raviart-Thomas MFE. To obtain accurate error estimates, we first rewrite the cell-centered FV scheme as a mixed variational formulation with certain numerical quadrature rules. We then carry out a standard adjoint-based analysis for the resultant mixed formulation. The estimate consists of residual errors from finite element approximation and quadrature errors. Numerical examples are presented which confirm the equivalence of the two numerical schemes and the accuracy of the *a posteriori* estimate.

8. Details of the analysis.

TABLE 6.5

Estimator in (5.5) and a bound obtained by taking absolute values of terms on each cell and then summing over the domain.

grid level	estimator	bound
1	-0.1096e+3	0.1096e+3
2	-0.3020e+2	0.3020e+2
3	-0.2201e+2	0.2201e+2
4	-0.2453e-1	0.4486e+1
5	-0.3167e-2	0.2082e+1
6	-0.6828e-3	0.6234e+0

8.1. Derivation of the cell-centered finite volume scheme. Using the divergence theorem to integrate the first equation of (2.1) over “volume” K_{ij} , we find

$$\begin{aligned}
& - \int_{y_{j-1/2}}^{y_{j+1/2}} a(x_{i+1/2}, y) p_x(x_{i+1/2}, y) dy + \int_{y_{j-1/2}}^{y_{j+1/2}} a(x_{i-1/2}, y) p_x(x_{i-1/2}, y) dy \\
& - \int_{x_{i-1/2}}^{x_{i+1/2}} a(x, y_{j+1/2}) p_y(x, y_{j+1/2}) dx + \int_{x_{i-1/2}}^{x_{i+1/2}} a(x, y_{j-1/2}) p_y(x, y_{j-1/2}) dx \quad (8.1) \\
& - \int_{x_{i-1/2}}^{x_{i+1/2}} \int_{y_{j-1/2}}^{y_{j+1/2}} (\beta^x p)_x + (\beta^y p)_y dx dy = \int_{x_{i-1/2}}^{x_{i+1/2}} \int_{y_{j-1/2}}^{y_{j+1/2}} f(p(x, y)) dx dy.
\end{aligned}$$

The right hand side can be approximated by $f_{ij} \Delta x_i \Delta y_j = f(p(x_i, y_j)) \Delta x_i \Delta y_j$, where f_{ij} is the value of f at (x_i, y_j) .

Since the first four terms on the left hand side can be treated in a similar fashion, we only show the procedure for approximating the first integral on interior cells which is

$$\begin{aligned}
\int_{y_{j-1/2}}^{y_{j+1/2}} a(x_{i+1/2}, y) p_x(x_{i+1/2}, y) dy & \approx \int_{y_{j-1/2}}^{y_{j+1/2}} a(x_{i+1/2}, y) \frac{p(x_{i+1}, y) - p(x_i, y)}{\Delta x_{i+1/2}} dy \\
& \approx a(x_{i+1/2}, y_j) \frac{p_{i+1,j} - p_{i,j}}{\Delta x_{i+1/2}} \Delta y_j.
\end{aligned}$$

Note that we have made two approximations at this step. Firstly, a piecewise constant approximation to the y -dependence of $a(x, y)$. Along each volume boundary we have replaced $a(x_{i+1/2}, y)$ by the midpoint (in y) value $a(x_{i+1/2}, y_j)$. Secondly, we have made a linear approximation to the x -dependence of p . If we denote the approximation to $p_x(x_{i+1/2}, y_j)$ as $\delta_x p_{i+1/2,j}$ and the approximation to $p_y(x_i, y_{j+1/2})$ as $\delta_y p_{i,j+1/2}$, then we have

$$\delta_x p_{i+1/2,j} = \frac{p_{i+1,j} - p_{i,j}}{\Delta x_{i+1/2}} \quad \text{and} \quad \delta_y p_{i,j+1/2} = \frac{p_{i,j+1} - p_{i,j}}{\Delta y_{j+1/2}} \quad (8.2)$$

on interior cells. We will extend this definition to cells adjacent to the outer boundary following the discussion of boundary conditions.

For a uniform mesh, the convection term is approximated as

$$\begin{aligned}
& \int_{x_{i-1/2}}^{x_{i+1/2}} \int_{y_{j-1/2}}^{y_{j+1/2}} (\boldsymbol{\beta}^x p)_x + (\boldsymbol{\beta}^y p)_y \, dx dy \\
&= \int_{y_{j-1/2}}^{y_{j+1/2}} \left(\int_{x_{i-1/2}}^{x_{i+1/2}} (\boldsymbol{\beta}^x p)_x \, dx \right) dy + \int_{x_{i-1/2}}^{x_{i+1/2}} \left(\int_{y_{j-1/2}}^{y_{j+1/2}} (\boldsymbol{\beta}^y p)_y \, dy \right) dx \\
&= \int_{y_{j-1/2}}^{y_{j+1/2}} (\boldsymbol{\beta}^x p)(x_{i+1/2}, y) - (\boldsymbol{\beta}^x p)(x_{i-1/2}, y) \, dy \\
&\quad + \int_{x_{i-1/2}}^{x_{i+1/2}} (\boldsymbol{\beta}^y p)(x, y_{j+1/2}) - (\boldsymbol{\beta}^y p)(x, y_{j-1/2}) \, dx \\
&\approx \Delta y_j \left(\boldsymbol{\beta}_{i+1/2,j}^x \hat{p}_{i+1/2,j} - \boldsymbol{\beta}_{i-1/2,j}^x \hat{p}_{i-1/2,j} \right) \\
&\quad + \Delta x_i \left(\boldsymbol{\beta}_{i,j+1/2}^y \hat{p}_{i,j+1/2} - \boldsymbol{\beta}_{i,j-1/2}^y \hat{p}_{i,j-1/2} \right),
\end{aligned}$$

where \hat{p} represents the approximation to the pressure on cell edges and is defined in (8.3). In the above formulation we make a piecewise constant approximation to $\boldsymbol{\beta}^x$ in direction y and a piecewise constant approximation to $\boldsymbol{\beta}^y$ in direction x . Here \hat{p} is defined as

$$\begin{aligned}
\hat{p}_{i,j-1/2} &= \frac{p_{i,j-1} + p_{i,j}}{2}, \quad 1 \leq i \leq k, \quad 2 \leq j \leq \ell, \\
\hat{p}_{i-1/2,j} &= \frac{p_{i-1,j} + p_{i,j}}{2}, \quad 2 \leq i \leq k, \quad 1 \leq j \leq \ell, \\
\hat{p}_{1/2,j} &= p_{1,j}, \quad \hat{p}_{k+1/2,j} = p_{k,j}, \quad 1 \leq j \leq \ell, \\
\hat{p}_{i,1/2} &= p_{i,1}, \quad \hat{p}_{i,\ell+1/2} = p_{i,\ell}, \quad 1 \leq i \leq k.
\end{aligned} \tag{8.3}$$

That is, if an edge is interior to the domain, \hat{p} is the average of pressure approximation in its adjacent cells in the case of uniform mesh. (Otherwise, average weighted by the sizes of neighbor cells is required). If an edge is on the outer boundary, \hat{p} is the value of the pressure approximation in the cell to which the edge belongs.

To enforce the boundary conditions, a standard approach is to make use of ghost cells with ghost values defined as

$$\begin{aligned}
p_{0,j} &= 2(\mathfrak{g}_D)_{1/2,j} - p_{1,j}, \quad p_{i,0} = 2(\mathfrak{g}_D)_{i,1/2} - p_{i,1}, \\
-a_{k+1/2,j} \frac{p_{k+1,j} - p_{k,j}}{\Delta x_{k+1/2}} &= (\mathfrak{g}_N)_{k+1/2,j}, \\
-a_{i,\ell+1/2} \frac{p_{i,\ell+1} - p_{i,\ell}}{\Delta y_{\ell+1/2}} &= (\mathfrak{g}_N)_{i,\ell+1/2},
\end{aligned} \tag{8.4}$$

where $1 \leq i \leq k$, $1 \leq j \leq \ell$. The terms $\Delta x_{k+1/2}$ and $\Delta y_{\ell+1/2}$ are defined due to the existence of ghost cells. An equivalent formulation to introducing ghost cells along Γ_N is to introduce edge pressure approximation λ^{FV} , which is constant and satisfies that, for $1 \leq i \leq k$, $1 \leq j \leq \ell$,

$$\begin{aligned}
-a_{k+1/2,j} \frac{\lambda_{k+1/2,j}^{\text{FV}} - p_{k,j}}{(\Delta x_{k+1/2}/2)} &= (\mathfrak{g}_N)_{k+1/2,j}, \\
-a_{i,\ell+1/2} \frac{\lambda_{i,\ell+1/2}^{\text{FV}} - p_{i,\ell}}{(\Delta y_{\ell+1/2}/2)} &= (\mathfrak{g}_N)_{i,\ell+1/2}.
\end{aligned} \tag{8.5}$$

We see that the edge pressure approximation λ^{FV} is the average of the pressure in the adjacent cell and the pressure in the ghost cell defined by (8.4). This alternative auxiliary variable is used to facilitate comparison of boundary conditions between mixed finite element and finite volume methods in Section 4. With this notation, we now complete the definitions of $\delta_x p$ and $\delta_y p$ as

$$\begin{aligned}\delta_x p_{1/2,j} &= \frac{p_{1,j} - (\mathbf{g}_D)_{1/2,j}}{\Delta x_{1/2}/2}, & \delta_x p_{k+1/2,j} &= \frac{\lambda_{k+1/2,j}^{\text{FV}} - p_{k,j}}{\Delta x_{k+1/2}/2}, & 1 \leq j \leq \ell, \\ \delta_y p_{i,1/2} &= \frac{p_{i,1} - (\mathbf{g}_D)_{i,1/2}}{\Delta y_{1/2}/2}, & \delta_y p_{i,\ell+1/2} &= \frac{\lambda_{i,\ell+1/2}^{\text{FV}} - p_{i,\ell}}{\Delta y_{\ell+1/2}/2}, & 1 \leq i \leq k.\end{aligned}\tag{8.6}$$

Combining all above results, we obtain (3.1).

8.2. Proof of Lemma 4.1. We first observe that, for piecewise polynomial spaces introduced in Section 2,

$$\begin{aligned}\mathfrak{M}_0^1(\Delta_x) &= \{s_{i+1/2}^x : 0 \leq i \leq k\} : & s_{i+1/2}^x(x_{\ell+1/2}) &= \delta_{i\ell}; \\ \mathfrak{M}_{-1}^0(\Delta_x) &= \{t_{i+1/2}^x : 1 \leq i \leq k\} : & t_{i+1/2}^x(x) &= 1, \text{ if } x_{i-1/2} < x < x_{i+1/2}; \\ \mathfrak{M}_0^1(\Delta_y) &= \{s_{j+1/2}^y : 0 \leq j \leq \ell\} : & s_{j+1/2}^y(y_{\ell+1/2}) &= \delta_{j\ell}; \\ \mathfrak{M}_{-1}^0(\Delta_y) &= \{t_{j+1/2}^y : 1 \leq j \leq \ell\} : & t_{j+1/2}^y(y) &= 1, \text{ if } y_{j-1/2} < y < y_{j+1/2}.\end{aligned}$$

Here, s represents piecewise linear function while t represents piecewise constant function. Note that s are scaled so as to be one at volume boundaries, not at the mid-points. Denote $\mathbf{u}_{h,i+1/2,j} = \mathbf{u}_h(x_{i+1/2}, y_j)$ and $p_{h,i,j} = p_h(x_i, y_j)$. The analysis is made according to three parts as follows.

I) Equation (2.4b) and (3.2c) : For equation (3.2c) with \mathbf{u}_h and p_h

$$\Delta x_i \Delta y_j \frac{\mathbf{u}_{h,i+1/2,j}^x - \mathbf{u}_{h,i-1/2,j}^x}{\Delta x_i} + \Delta x_i \Delta y_j \frac{\mathbf{u}_{h,i,j+1/2}^y - \mathbf{u}_{h,i,j-1/2}^y}{\Delta y_j} = f_{ij} \Delta x_i \Delta y_j,$$

both $\frac{\partial \mathbf{u}_h^x}{\partial x}$ and $\frac{\partial \mathbf{u}_h^y}{\partial y}$ are constants on each volume, so we have

$$\int_{x_{i-1/2}}^{x_{i+1/2}} \int_{y_{j-1/2}}^{y_{j+1/2}} \nabla \cdot \mathbf{u}_h \, dy \, dx = \Delta x_i \Delta y_j \frac{\partial \mathbf{u}_h^x}{\partial x} + \Delta x_i \Delta y_j \frac{\partial \mathbf{u}_h^y}{\partial y}.$$

Hence, for any $w \in W_h$,

$$(\nabla \cdot \mathbf{u}_h, w) = (f, w)_{M_x M_y}.\tag{8.7}$$

This corresponds to equation (2.4b) for the lowest order Raviart-Thomas mixed finite element scheme. Here, M_x and M_y are midpoint quadratures in x- and y- directions. We also denote the trapezoidal quadratures in x- and y-directions by T_x and T_y respectively.

II) Equation (2.4a) and (3.2a), (3.2b) for interior cells : Multiplying (3.2a) in terms of \mathbf{u}_h and p_h by $\frac{1}{2}(\Delta x_i + \Delta x_{i+1})\Delta y_j a_{i+1/2,j}^{-1} = \Delta x_{i+1/2}\Delta y_j a_{i+1/2,j}^{-1}$, we obtain

$$\begin{aligned}\frac{1}{2}(\Delta x_i + \Delta x_{i+1})\Delta y_j (a_{i+1/2,j})^{-1} \mathbf{u}_{h,i+1/2,j}^x - \Delta y_j (p_{h,i,j} - p_{h,i+1,j}) \\ + \mathbf{b}_{i+1/2,j}^x \frac{p_{h,i+1,j} + p_{h,i,j}}{2} \Delta x_{i+1/2} \Delta y_j = 0.\end{aligned}$$

For a test function $\mathbf{v} = (s_{i+1/2}^x t_{j+1/2}^y, t_{i+1/2}^x s_{j+1/2}^y)$ with

$$\begin{aligned} s_{i+1/2}^x &\in \mathfrak{M}_0^1(\Delta_x), & t_{j+1/2}^y &\in \mathfrak{M}_{-1}^0(\Delta_y), \\ t_{i+1/2}^x &\in \mathfrak{M}_{-1}^0(\Delta_x), & s_{j+1/2}^y &\in \mathfrak{M}_0^1(\Delta_y), \end{aligned}$$

the above equation can be written as

$$\begin{aligned} \left(a^{-1} \mathbf{u}_h^x, s_{i+1/2}^x t_{j+1/2}^y \right)_{T_x M_y} - \left(p_h, \frac{\partial}{\partial x} \left(s_{i+1/2}^x t_{j+1/2}^y \right) \right) \\ + \left(\mathbf{b}^x p_h, s_{i+1/2}^x t_{j+1/2}^y \right)_{T_x M_y} = 0, \end{aligned}$$

since both \mathbf{u}_h^x and $(s_{i+1/2}^x t_{j+1/2}^y)$ are functions that are continuous linear in x and discontinuous piecewise constant in y and $\frac{\partial}{\partial x} (s_{i+1/2}^x t_{j+1/2}^y)$ is discontinuous piecewise constant in x and y . Recall that p_h is piecewise constant.

Similarly, from (3.2b) we have

$$\begin{aligned} \left(a^{-1} \mathbf{u}_h^y, t_{i+1/2}^x s_{j+1/2}^y \right)_{M_x T_y} - \left(p_h, \frac{\partial}{\partial y} \left(t_{i+1/2}^x s_{j+1/2}^y \right) \right) \\ + \left(\mathbf{b}^y p_h, t_{i+1/2}^x s_{j+1/2}^y \right)_{M_x T_y} = 0. \end{aligned}$$

Summing the two equations, we obtain

$$\begin{aligned} \left(a^{-1} \mathbf{u}_h^x, \mathbf{v}^x \right)_{T_x M_y} + \left(a^{-1} \mathbf{u}_h^y, \mathbf{v}^y \right)_{M_x T_y} - (p_h, \nabla \cdot \mathbf{v}) \\ + (\mathbf{b}^x p_h, \mathbf{v}^x)_{T_x M_y} + (\mathbf{b}^y p_h, \mathbf{v}^y)_{M_x T_y} = 0, \quad \forall \mathbf{v} \in V_h. \end{aligned} \quad (8.8)$$

III) Cells adjacent to the boundary : We compare (2.4a) and (3.2a), (3.2b) and compare (2.4c) and (3.3) in cells adjacent to the boundaries.

Neumann boundary: On a Neumann boundary edge e , (3.3) can be written as

$$\langle \mathbf{u}_h \cdot \mathbf{n} + \boldsymbol{\beta} \cdot \mathbf{n} \lambda^{\text{FV}}, \mu \rangle_{e, M} = \langle \mathfrak{g}_N, \mu \rangle_{e, M}, \quad \forall \mu \in P^0(e), \quad (8.9)$$

which corresponds to (2.4c). The subscript M indicates integration using the midpoint rule on a 1-D domain.

Consider a cell with an edge e along one of the Neumann boundaries, i.e., $K_{k+1/2, j}$ or $K_{i, \ell+1/2}$ for some $1 \leq j \leq \ell$ or $1 \leq i \leq k$. If $e \in K_{k+1/2, j}$, multiplying (3.2a) at $i = k$ by $\frac{1}{2}(\Delta x_{k+1/2})\Delta y_j a_{k+1/2, j}^{-1} = \frac{1}{2}\Delta x_k \Delta y_j a_{k+1/2, j}^{-1}$, we obtain

$$\begin{aligned} \frac{1}{2} a_{k+1/2, j}^{-1} \mathbf{u}_{h, k+1/2, j}^x \Delta x_{k+1/2} \Delta y_j - p_{h, k, j} \Delta y_j + \frac{1}{2} \mathbf{b}_{k+1/2, j}^x p_{h, k, j} \Delta x_{k+1/2} \Delta y_j \\ + \lambda_{k+1/2, j}^{\text{FV}} \Delta y_j = 0. \end{aligned}$$

For test function $\mathbf{v} = (s_{k+1/2}^x t_j^y, t_{k+1/2}^x s_j^y)^\top$, this can be rewritten as

$$\left(a^{-1} \mathbf{u}_h^x, \mathbf{v}^x \right)_{T_x M_y} - \left(p_h, \frac{\partial \mathbf{v}^x}{\partial x} \right) + (\mathbf{b}^x p_h, \mathbf{v}^x)_{T_x M_y} + \langle \lambda^{\text{FV}}, \mathbf{v}^x \mathbf{n}^x \rangle_{\Gamma_N} = 0. \quad (8.10)$$

Dirichlet boundary: Similarly, for cells containing an edge along one of the Dirichlet boundaries, e.g., $e = (x_{i-1/2}, x_{i+1/2}) \times \{y_{1/2}\}$, we derive

$$(a^{-1}\mathbf{u}_h^y, \mathbf{v}^y)_{M_x T_y} - \left(p_h, \frac{\partial \mathbf{v}^y}{\partial y} \right) + (\mathbf{b}^y p_h, \mathbf{v}^y)_{M_x T_y} = - \langle \mathbf{g}_D, \mathbf{v}^y \mathbf{n}^y \rangle_{\Gamma_D, M}. \quad (8.11)$$

Collating (8.8), (8.10) and (8.11), we obtain a weak formulation for the finite volume method in the form of (2.3a), namely

$$(a^{-1}\mathbf{u}_h^x, \mathbf{v}^x)_{T_x M_y} + (a^{-1}\mathbf{u}_h^y, \mathbf{v}^y)_{M_x T_y} - (p_h, \nabla \cdot \mathbf{v}) + \langle \lambda^{\text{FV}}, \mathbf{v} \cdot \mathbf{n} \rangle_{\Gamma_N} + (\mathbf{b}^x p_h, \mathbf{v}^x)_{T_x M_y} + (\mathbf{b}^y p_h, \mathbf{v}^y)_{M_x T_y} = - \langle \mathbf{g}_D, \mathbf{v} \cdot \mathbf{n} \rangle_{\Gamma_D, M}. \quad (8.12)$$

It is easy to verify that λ^{FV} on Neumann boundary edges plays the same role as the Lagrange multiplier λ_h in the mixed finite element method. From now on, we abuse the notation of λ^{FV} and λ_h .

Collecting all the terms, we obtain (4.1), which is an equivalent mixed finite element method for finite volume scheme (3.1).

REFERENCES

- [1] Y. ACHDOU, C. BERNARDI, AND F. COQUEL, *A priori and a posteriori analysis of finite volume discretizations of Darcy's equations*, Numer. Math., 96 (2003), pp. 17–42.
- [2] M. AFIF, A. BERGAM, Z. MGHAZLI, AND R. VERFÜRTH, *A posteriori estimators for the finite volume discretization of an elliptic problem*, in International Conference on Numerical Algorithms, Vol II (Marrakesh 2001). Numer. Algorithms 34, no. 2-4, 2003, pp. 127–136.
- [3] A. AGOUZAL AND F. OUDIN, *A posteriori error estimator for finite volume methods*, Appl. Math. Comput., 110 (2000), pp. 239–250.
- [4] T. ARBOGAST, M.F. WHEELER, AND I. YOTOV, *Mixed finite elements for elliptic problems with tensor coefficients as cell-centered finite differences*, SIAM J. Num. Anal., 34 (1997), pp. 828–852.
- [5] WOLFGANG BANGERTH AND ROLF RANNACHER, *Adaptive Finite Element Methods for Differential Equations*, Birkhauser Verlag, 2003.
- [6] J. BARANGER, J.-F. MAITRE, AND F. OUDIN, *Connection between finite volume and mixed finite element methods*, RAIRO Modél. Math. Anal. Numér., 30 (1996), pp. 445–465.
- [7] T. J. BARTH, *A posteriori error estimation and mesh adaptivity for finite volume and finite element methods*, in Springer series Lecture Notes in Computational Science and Engineering, vol. 41, Springer, New York, 2004.
- [8] R. BECKER AND R. RANNACHER, *An optimal control approach to a posteriori error estimation in finite element methods*, Acta Numerica, (2001), pp. 1–102.
- [9] F. BREZZI AND M. FORTIN, *Mixed and Hybrid finite element methods*, Springer-Verlag, New York, 1991.
- [10] C. CARSTENSEN, R. LAZAROV, AND S. TOMOV, *Explicit and averaging a posteriori error estimates for adaptive finite volume methods*, SIAM J. Numer. Anal., 42 (2005), pp. 2496–2521.
- [11] P. CASTILLO, *An a posteriori error estimate for the local discontinuous Galerkin method*, SIAM J. Sci. Comput., 22/23 (J. Sci. Comput.), pp. 187–204.
- [12] K. ERIKSSON, D. ESTEP, P. HANSBO, AND C. JOHNSON, *Introduction to adaptive methods for differential equations*, in Acta numerica, 1995, Acta Numer., Cambridge Univ. Press, Cambridge, 1995, pp. 105–158.
- [13] ———, *Computational differential equations*, Cambridge University Press, Cambridge, 1996.
- [14] D. ESTEP, *A posteriori error bounds and global error control for approximation of ordinary differential equations*, SIAM J. Numer. Anal., 32 (1995), pp. 1–48.
- [15] D. ESTEP, *A short course on duality, adjoint operators, Green's functions, and a posteriori error analysis*, 2004. Sandia National Laboratories, Albuquerque, New Mexico. Notes can be downloaded from <http://math.colostate.edu/~estep>.
- [16] D. ESTEP, M. G. LARSON, AND R. D. WILLIAMS, *Estimating the error of numerical solutions of systems of reaction-diffusion equations*, Mem. Amer. Math. Soc., 146 (2000), pp. viii+109.
- [17] R. EYMARD, T. GALLOUËT, AND R. HERBIN, *Finite volume methods*, in Handbook of numerical analysis, vol. VII, North-Holland, Amsterdam, 2000, pp. 713–1020.

- [18] M. GILES AND E. SÜLI, *Adjoint methods for PDEs: A posteriori error analysis and postprocessing by duality*, Acta Numerica, (2002), pp. 145–236.
- [19] R. HERBIN AND M. OHLBERGER, *A posteriori error estimate for finite volume approximations of convection-diffusion problems*, in Proceedings of the 3rd International Symposium on: Finite Volumes For Complex Applications - Problems and Perspectives, 2002.
- [20] JR J. DOUGLAS AND J.E. ROBERTS, *Mixed finite element methods for second order elliptic problems*, Mat. Aplic. Comp., 1 (1982), pp. 91–103.
- [21] M. G. LARSON AND T. J. BARTH, *A posteriori error estimation for adaptive discontinuous Galerkin approximations of hyperbolic systems*, in Discontinuous Galerkin Methods, Cockburn, Karniadakis, and Shu, eds., vol. 11 of Lecture Notes in Computational Science and Engineering, Springer-Verlag, New York, 1999.
- [22] ———, *A-posteriori error estimation for higher order Godunov finite volume methods on unstructured meshes*, in Finite Volumes for Complex Applications III, Herbin and Kroner, eds., Hermes Science Pub., London, 2002, pp. 41–63.
- [23] P. D. LAX, *Weak solutions of nonlinear hyperbolic equations and their numerical computation*, Comm. Pure Appl. Math., 7 (1954), pp. 159–193.
- [24] P. D. LAX AND B. WENDROFF, *Systems of conservation laws*, Comm. Pure Appl. Math., 13 (1960), pp. 217–237.
- [25] S. NICAISE, *A posteriori error estimations of some cell-centered finite volume methods*, SIAM J. Numer. Anal., 43 (2005), pp. 1481–1503.
- [26] ———, *A posteriori error estimations of some cell centered finite volume methods for diffusion-convection-reaction problems*, SIAM J. Numer. Anal., 44 (2006), pp. 949–978.
- [27] J. T. ODEN AND S. PRUDHOMME, *Goal-oriented error estimation and adaptivity for the finite element method*, Comput. Math. Appl., 41 (2001), pp. 735–756.
- [28] T. F. RUSSELL AND M. F. WHEELER, *Finite element and finite difference methods for continuous flows in porous media*, in The Mathematics of Reservoir Simulation, R. E. Ewing, ed., SIAM, Philadelphia, 1983.
- [29] M. VOHRALIK, *Residual flux-based a posteriori error estimates for finite volume and related locally conservative methods*, Numer. Math (to appear).
- [30] ———, *Two types of guaranteed (and robust) a posteriori estimates for finite volume methods*, in Proceedings of Finite Volumes for Complex Applications V, Eymard R. and Hrad J.-M., eds., ISTE and John Wiley & Sons, London, UK and Hoboken, USA, 2008.